SEMARAK ILMU PUBLISHING

CFD Letters

Journal homepage:
https://semarakilmu.com.my/journals/index.php/CFD_Letters/index
ISSN: 2180-1363

Investigation of Energy Dissipation for Different Breakwater Based on Computational Fluid Dynamic Model

Uday Abdul Sahib M. Alturfi[1,*], Abdul-Hassan K. Shukur[2]

[1] Faculty of Engineering, Department of Structures and Water Resources, University of Kufa, Najaf, Iraq
[2] Faculty of Engineering, Department of Civil Engineering, University of Babylon, Babylon, Iraq

ARTICLE INFO

Article history:
Received 16 May 2023
Received in revised form 14 June 2023
Accepted 18 July 2023
Available online 5 December 2023

Keywords:
CFD; Wave transmission; incident wave; numerical beach; VOF; Dynamic mesh; breakwater

ABSTRACT

In this research, the hydraulic performance of the combined shape breakwaters was investigated through a laboratory study supported by a numerical mathematical model CFD to examine the different model shapes depending on the transmissions wave coefficient Ct. In order to stabilize the incident wave Hi with the same characteristics, waves were defined through the UDF file for CFD model. To investigated the performance of breakwaters base on energy dissipations, different models were tested under various wave condition, water depth, and relative submerged depth. Result of this study are showed that the Transmission coefficient are increased with increased of incident wave high for all type of breakwater model, and for all models of breakwater, transmission wave height (H_t) are increased with increased relative submerged depth (Hs/Hi). The highest value for energy dissipations (1 - C_t) % are received for zero submerged depth in model of sloped steps model (M2) is 80 %. Ansys Fluent solver are adopted to modelling the transit flow condition with dynamic mesh to represent the flap motion type to generate wave. Numerical beach plays an important role in CFD model to prevent the reflection wave in lee side of breakwater and represent the absorbing shoreline. 240 grid per wave length are selected for Mesh independent solution and make acceptable result comparison with experimental.

1. Introduction

Breakwaters are the structures built to safeguard coastal infrastructure. These structures are essential in the hard climate conditions to combat the enormous power of the sea waves. Breakwaters are evaluated in terms of stability and energy dissipation capability in order to maintain their viability and comprehend their behavior when interacting with nature. In the current work, the energy dissipation capacity of breakwater is evaluated for various shapes using an experimental and numerical model [1].

Numerical simulations have a tendency to dominate scientific research because to the recent significant advancements in computing power, storage capacity, and calculation speed. To gain a deeper understanding of the behavior of systems whose mathematical models are too complicated

* *Corresponding author.*
E-mail address: oday.alturfi@uokufa.edu.iq (Uday Abdul Sahib M. Alturfi)

https://doi.org/10.37934/cfdl.16.1.2242

for analytical solutions; numerical simulations are being employed more often. This is true for the majority of non-linear systems, which itself best characterize most situations in real life. In cases when it is difficult to duplicate the in-situ conditions or where physical experimental procedures are more time- and money-consuming, computer-based simulations are given as an alternative. The gas and liquid interactions with surfaces that have been specified by boundary conditions is simulated using computational fluid dynamics (CFD). The Navier-Stokes equations serve as the essential foundation for practically all CFD issues [2].

One of the key components of a harbor's design is the selection of an appropriate breakwater. The choice of breakwater type is influenced by a number of variables, including wave height, wave period, water depth, characteristics of the sea bottom soil foundation, material that is readily accessible on the site or nearby, and building tools. Breakwaters are divided into four groups based on their structural characteristics: sloping (rubble mound), vertical, composite type breakwaters, and special (non-gravity) types of breakwaters like pile or pneumatic system [3].

Submerged breakwaters are extensively employed for the purpose of coastal protection owing to their ability to dissipate wave energy and mitigate coastal erosion. The dissipation of energy in the vicinity of submerged breakwaters can be attributed to two primary mechanisms, namely, wave breaking over the breakwaters and vortex generation on both sides of the submerged breakwaters.

In the present work, sloping, vertical, and non-conventional type (steps breakwater) are studies to demonstrated that the transmission coefficient associated with each type of breakwater according to experimental and CFD modeling approaches.

In this part of the research, a briefly and quickly review on the most important numerical and experimental studies on the use of breakwaters as a means of dispersing energy of wave incident. Historical studies on mitigation structures, also known as submerged breakwaters, have indicated that these structures influence a wide range of physical processes. Some factors, such as structural design, sloping ground stability, scour, wave transmission, and flow pattern, are extremely important. The transmission coefficient (Ct), which measures the ratio of the passing wave to the incident wave, is one of the most successful methods for designing a breakwater. Many researchers have focused their attention on the study of submerged breakwaters due to the importance of these structures in coastal protection.

Using a two-dimensional structure in the shape of a trapezium, Stucky and Bonnard [4] carried out the first known experiment in the physical realm to investigate wave transmission related to submerged breakwaters. The Beach Erosion Board [4] continued their research in more thorough 2D geometrical detail. Rectangular breakwaters were studied by Morison and Johnson *et al*., [4]. Longer period waves were often less impacted by breakwater crest width and height, according to Johnson *et al*., [4], who also demonstrated superior energy dissipation of steeper waves with a broader barrier.

For several types of breakwaters structures, Abdul Khader and Rai [5] calculated the coefficient of transmission C_t, or the ratio of transmitted to incident wave height. They came to the conclusion that, when compared to other varieties of submerged breakwaters, rectangular breakwaters are the most efficient in dissipating energy.

As previous studies, many researchers have dealt with this topic and some of them, Dougelass and Krolaak [6], Dick and Brebner [7], Seabrook and Hall [8], Calabrese [9], Tajziehchi [10], Liao, *et al*., [11], Replumaz *et al*., [12] and Al Shaikhli *et al.,* [13] Sharif [25], demonstrated a mathematical and experimental analysis of several forms of an inclined rubble mound breakwater. To examine the design of mound breakwaters in order to ascertain the breaking wave behavior, including transmission coefficient and energy dissipation. The velocity field and vortex formation around the submerged breakwaters were researched by Hsu *et al.,* [14] and Zhang *et al*., [15]. Young and Testik

[16], investigated the reflection and diffraction of waves from underneath breakwaters. Experimental research on wave breaking and energy loss over porous structure submerged breakwater was conducted by Liao *et al*., [17]. In 2012 and 2014, Hajivalie and Yeganeh-Bakhtiary, [18] researched the scouring around a rectangular underwater breakwater. Hajivalie *et al*., [18] investigated the impact of vertical breakwater size on transmission coefficient and vortex production around the breakwaters using a RANS equation based computational model in conjunction with a conventional k-model. They came to the conclusion that extending the breakwater width would not significantly improve wave energy dissipation by the breakwater unless it is wider than a specific rate, which may vary depending on the relative submergence depth. They clarify that at this particular breadth, the vertical submerged breakwater is not subject to wave breaking. This discovery casts doubt on earlier predictions that the vertical breakwater may dissipate more wave energy than other submerged breakwater shapes, such as trapezoidal and semicircular, in every situation.

In summary, the selection of breakwater shape depends on various factors such as wave energy dissipation (transmission coefficient), stability, cost, and environmental impact. The choice of shape should be based on a careful analysis of these factors to ensure that the breakwater is effective, efficient, and sustainable. In the present work, the breakwater shape is choosing according to most effect and sufficient to dissipated more energy (low transmission coefficient).

According to the previous studies on the breakwater, it can be found that the subject of studying the compound breakwater (sloped steps) in comparison with other types has not been clearly studied by researchers, in addition, this model was represented using CFD modeling

2. Experiment Set-up Specifications

2.1 Wave Flumes

The hydraulic laboratory of the Faculty of Engineering, University of Kufa-Iraq, has a 2D-wave flume where the physical model studies are conducted. Didacta Italia manufactured the flume to investigate the hydrodynamic characteristics of open surface streams in channels with different angles of inclination. The wave generator used in the experiment is a bottom-hinged paddle design capable of creating predictable monochromatic waves. The waves created by the wave paddle run through thin vertical sheets of asbestos to provide turbulence-free, smooth waves. The wave flume contains active wave absorption that may take in the test model's reflected wave. The channel is composed of tempered glass, section 0.3 m x 0.45 m, length 15 m. flume include with wave maker submerged blade type, an electric motor with a variable speed serves as its controller (see Figure 1).

Fig. 1. Open surface tilting flow Channel

It is a wave maker of the submerged blade type, and it is operated by an electric motor with variable speed. It enables one to see the form of the waves as they travel through a channel. Specification of wave tank flume: Ratio-motor: speed ratio 1:30, max speed 47 rpm, absorbed power: 0.12 kW. Inverter for revolution speed regulation Figure 2 shows the wave generator and absorbing beach in flume.

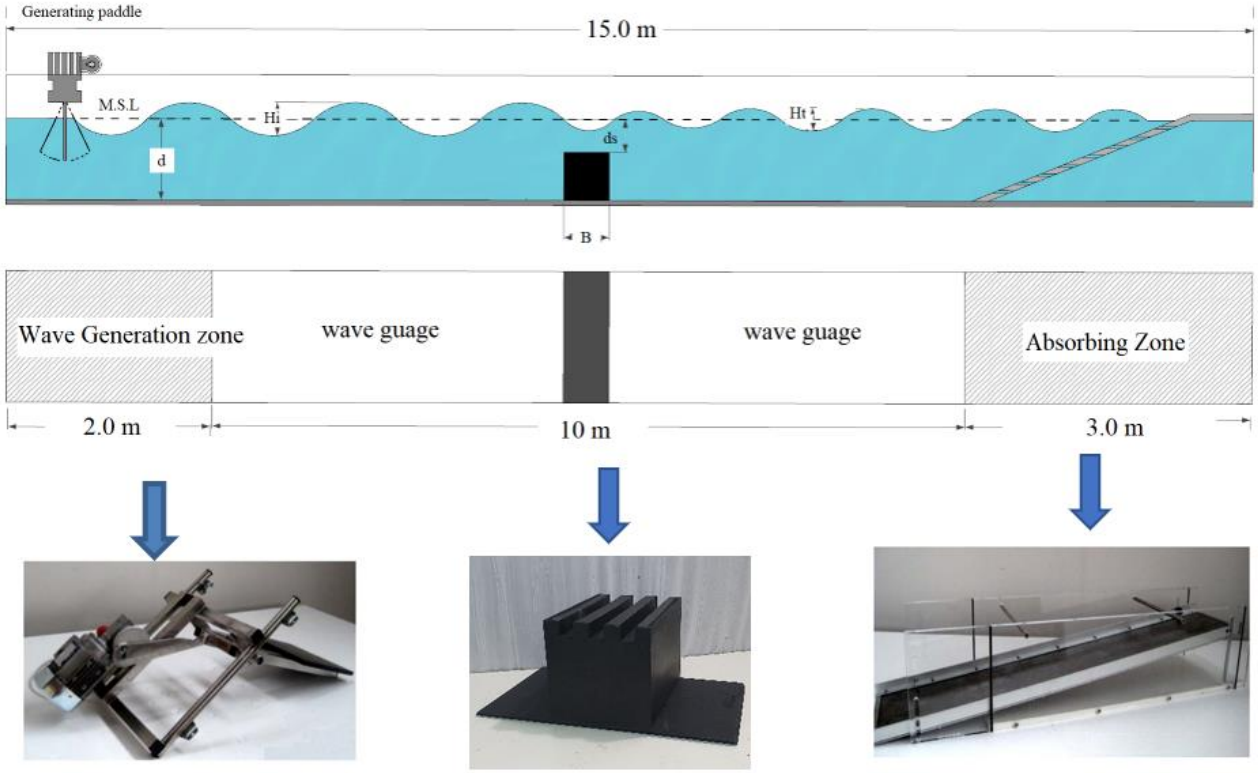

Fig. 2. Flume with step-up of wavemaker, model test, and absorbing device

2.2 Wave Tank modelling

Discussing the CFD modelling of an experimental research employing various methods of surface wave generation on a tank (piston and flap type wavemaker) is one of the goals of this study. For various boundary conditions, some computer simulations of these processes have been created. The wave tank is roughly represented in Figure 3.

2.3 Wavemaker Theory

A wavemaker produces waves by oscillating a mechanical component within the wavemaker. The two kinds of wavemakers that are often distinguished are flap and piston. For experiments in shallow water, a piston-type wavemaker is utilized. Modelling buildings along the shore, harbour, etc. uses this form of generator because the piston motion limits the particle orbital motion to an ellipse. Galvin put up a straightforward wavemaker idea in 1964 [3]. The particle orbital motion in a wavemaker of the flap type decreases with depth and becomes insignificant at the bottom, Figure 3.

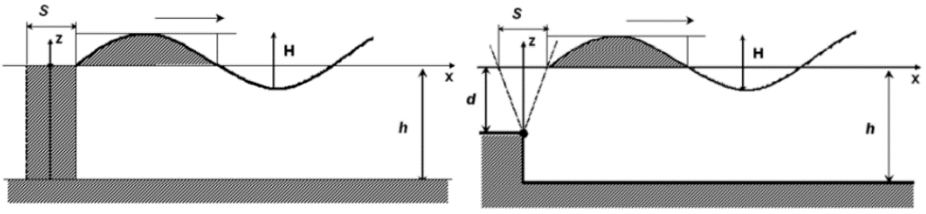

(a) Piston type wavemaker (b) flap type wavemaker

Fig. 3. wavemaker type according to mechanics of movement

According to Galvin's hypothesis for flap-type wavemakers, when the piston has a stroke of S with depth h, the volume of water displaced will be S h. A wave crest's water volume may be calculated using the formula of Eq. (1) [24].

$$\int_0^{\frac{\lambda}{2}} \left(\frac{H}{2}\right) sin\, kx\, dx = \frac{H}{k} \tag{1}$$

consideration the volumes into both sides, the following expression become as

$$SH = \frac{H}{k} = \frac{H}{2}\left(\frac{\lambda}{2}\right)\frac{2}{\pi} \tag{2}$$

In Figure (3), the shaded area corresponds to the factor 2/ π. The straightforward wavemaker hypothesis for a piston is as follows:

$$\left(\frac{H}{s}\right) = kh \tag{3}$$

where H/S stands for the shallow water-appropriate height to stroke ratio (shallow water condition kh < π/10). The wavemaker theory is complete when boundary conditions are taken into account, and the following formula for wave height to stroke is derived.

$$\frac{H}{s} = \frac{2\left(cos\, 2k_p h - 1\right)}{sinh\, 2kph + 2k_p h} \tag{4}$$

H; represent height of wave: and the progressive wavenumber is denoted by k_p.

In the present study, according to the flume experimental flap type wavemakers are generally used for investigating and generating water waves, Figure 4. When the flap wavemaker is hinged at the bottom, the expression is:

$$\left(\frac{H}{S}\right) = \frac{kh}{2} \tag{5}$$

The wave height to stroke ratio of the flap type wavemaker changes to Eq. (6) when boundary circumstances are taken into account.

$$\frac{H}{s} = 4\left(\frac{sinh\, kph}{\overline{k_P h}}\right)\frac{k_p h\, sin\, hkPh - cosh\, kph + 1}{sin\, h2k_p h + 2k_P h} - \tag{6}$$

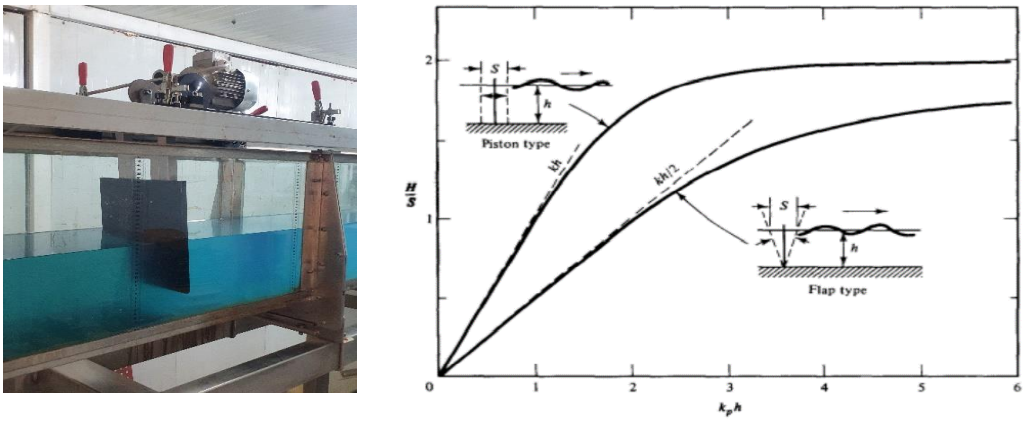

Fig. 4. Flap type wavemaker snapshot

2.4 Model Set-up and Geometry

The model studies were primarily used to understand how the transmission coefficient varies with regard to regular wave conditions such as: shape of breakwater: incident wave height: wave steepness, transmission coefficient for each type. Figure 5 represent the model installed in flume and all parameters for breakwater and wave conditions.

Where: H = Wave height, Hi = Incident wave height, Ht = Transmission wave, h= Stall water high SWL, Hs = Submerge depth, LB = Length of breakwater, and HB= height breakwater.

Five model are used to test the wave transmission coefficient, these models are organized according to the shape of cross section as showing in Figure 6. These models are manufactured from moisture-resistant plastic materials using machinery 3D printing for very fine details, Figure 6

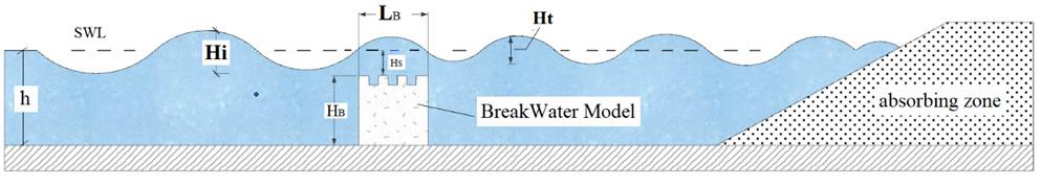

Fig. 5. Sketch of Breakwater model and specification

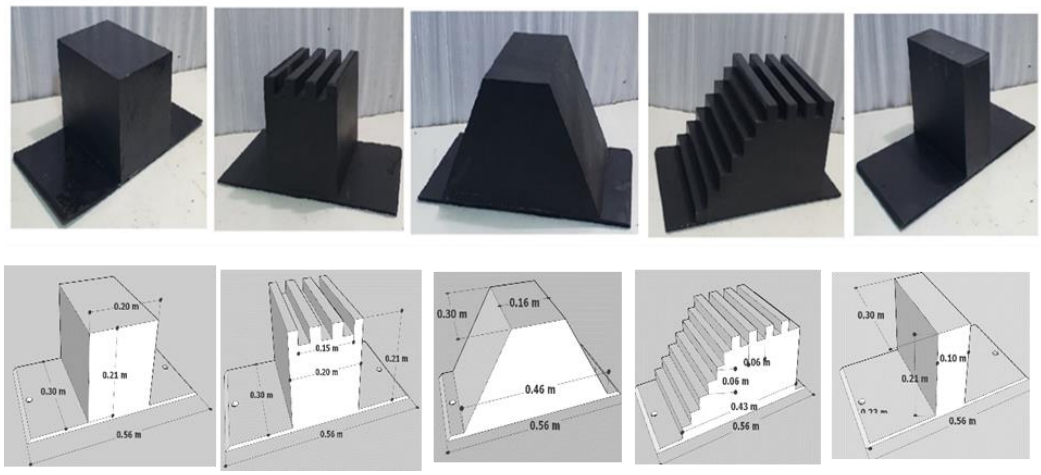

Fig. 6. Physical Models with dimensions

2.5 Hydraulic Parameters of Breakwater

Table 1 demonstrated the hydraulic characteristics that characterized the physical research, breakwater shape, and wave conditions. Each experiment test repeated three times to get the average of each run, so that the total number of experiments was 150 tests as shown in table. During experiments, the incident surface heights of the waves are measured using wave measurement device positioned at a distance of one wave length L. The wave Transmission coefficient (Ht) is computed using the collected data. By first assigning a regular wave motion in the wave flume using a UDF (user-defined function) with the movement of the flap-type paddle, the formation of waves is started under hydrostatic circumstances (water at rest) of the flume. Making the computational space into a limited number of a control volume allows for the solution of the governing equations (conservation of mass and moment). The liquid face is given a static pressure as a starting condition, and the free surface between the air and water medium is created using the fluid model's volume.

Table 1
Hydraulic parameters breakwater modelling

Model breakwater	Symbols	Submerged Depth (Hs) cm	incident wave elevations	Motor Speed Ratio max speed 47 RPM
Rubble mound	M1	0, 4, 9, 13, 15	10, 12,15	20, 30
Sloped with steps	M2			
Rectangular	M3			
Rectangular with steps	M4			
Rectangular narrow	M5			

3. Computational Fluid Dynamic

The field of Computational Fluid Dynamics (CFD) involves the utilisation of mathematical and physical problem formulation techniques, as well as numerical methods such as discretization methods, solvers, numerical parameters, and grid generations, to simulate fluids engineering systems. The procedure is depicted in Figure 7. Pre-processing, processing, and post-processing comprise CFD. The problem statement is discretely modelled in pre-processing. Geometry, meshing, physics, and boundary conditions do this. Computers calculate fluid flow numerically. Post-processing analyses and displays findings [19].

CFD starts with find the best mathematical model that describes the problem, followed by specifying the computational domain of interest. Computational domain discretization is an early and essential step in almost all commercial numerical solution packages [20].

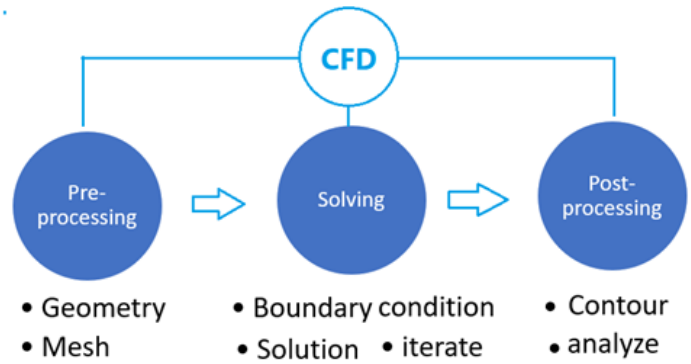

Fig. 7. CFD processing in three stages

3.1 Mathematical Model (Fluent solver)

In the current work, the Volume of Fluid (VOF) formulation in FLUENT is used to create the two-dimensional numerical model. The nonlinear and free surface flow motion of the wave is formulated using the Navier-Stokes Eq. (7) and the continuity Eq. (8). The water is assumed to be an incompressible Newtonian fluid whose density is constant across time.

$$\boldsymbol{\rho}\left(\frac{\boldsymbol{\partial w}}{\boldsymbol{\partial t}}+\boldsymbol{w\nabla w}\right)=-\boldsymbol{\nabla_P}+\boldsymbol{\nabla\mu(\nabla w)}+\boldsymbol{F} \tag{7}$$

$$\frac{\partial \mathrm{u}}{\partial \mathrm{x}}+\frac{\partial \mathrm{u}}{\partial \mathrm{y}}=0 \tag{8}$$

So basically, you've got w for fluid velocity, u and v for velocity in the x and y directions, p for fluid pressure, Z for fluid density, and μ for dynamic fluid viscosity. So, in Eq. (7), the first part is all about the forces that make things move; the second part is about pressure and other forces; the third part is about how sticky the fluid is; and the fourth part is about any outside forces acting on the fluid.

3.2 Boundary Condition

This stage of preparing the model is very important because it determines the extent to which the physical phenomenon (waves) can be represented phasic of wave correctly. In present work, Figure 8 shown the all the boundary condition had been used, the maintain zero velocity (no slip wall) on all the walls. Also, the pressure condition for outlet boundary at the top is set by default to zero gauge (or atmospheric). A pressure outlet was designated for the model top surface. Absolute pressure less ambient pressure is known as static pressure or gauge pressure. The open channel option is used in the velocity inlet to offer the SWL area, which is small (0.21 to 0.36 m). User Define Function (UDF) are used to model the wave condition in the zone of wave generation.

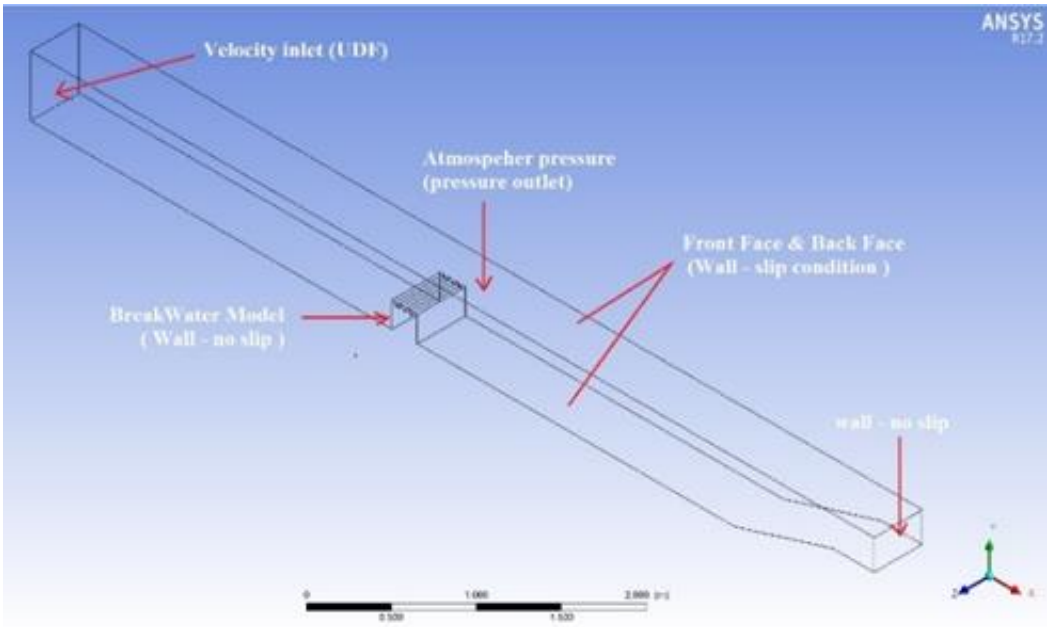

Fig. 8. Boundary condition description

3.3 Setup & VOF Model

The numerical model utilized is based on the Volume of Fluid (VOF) approach, which enables computational wave simulation by closely simulating the interaction of water and air. The transient is choosing of gravity-based model is used in this work. The volume fraction parameter is represented implicitly in the VOF model with open channel wave boundary conditions. Two-phase incompressible fluids (air and water) are used in the simulations, with constant densities of 998 kg/m3 for the water and 1.225 kg/m3 for the air. It is recommended to use K-omega viscous models for turbulent open channel flows [21]. The SST k-omega viscous model is used in this experiment to produce waves. The selection of wave boundary conditions and wave theory is influenced by wave steepness and relative water depth. The proper wave theories for different wave situations (shallow to deep sea) were described in DNV RP C 205 (2010), a suggested code practice, similar to FLUENT [22]. All numerical simulations at the velocity inlet are conducted with Stokes' third-order wave theory and a shallow/intermediate wave boundary condition.

3.4 Mesh Independence Solution

The precision and stability of the numerical calculation are significantly influenced by the mesh quality. Node point distribution, smoothness, and skewness are characteristics connected to mesh quality. (Ansys2010). Incorrect mesh selection can have an impact on simulation accuracy, computational efficiency, and solution stability. Several literature sources and studies have indicated that a model must be designed with a minimum of 200 grids per wavelength, as stated by Arun Kamath in 2012 [23]. Additionally, appropriate wave generation may be achieved if the aspect ratio of an element is less than 10, as suggested by Marques [23]. In the current work, a maximum element length of 0.005 m is required to create waves with a maximum wavelength of 1.5 m. As a result, all of the tests are run with a mesh size of $25*10^{-6}$ m^2 and an element aspect ratio of one, Figure 9 represent the mesh discretised.

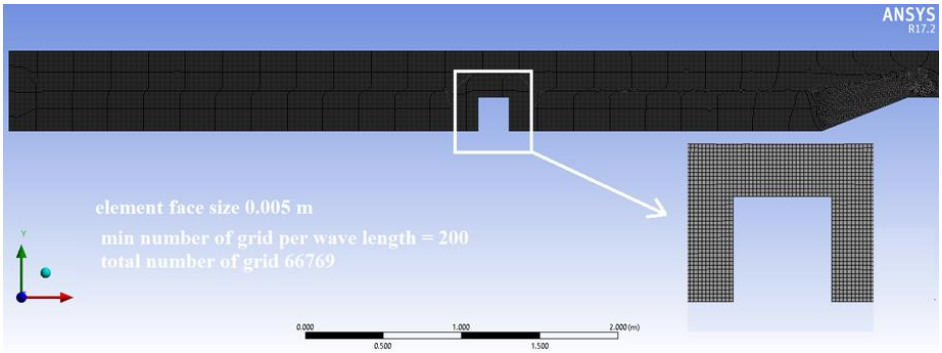

Fig. 9. mesh description and specification

Figure 10 depicts the fluctuation with transmission coefficient (Kt) for the region of interest for different grid sizes. The quality of the results is also affected by the temporal discretization and transient formulation utilized in the investigation. The grid sizes evaluated for present work are 0.004 m, 0.005 m, 0.006 m, 0.007 mm, and 0.008 mm. For 0.004 m and 0.005 m grid sizes (see Table 2), the mesh in depend solution is achieved, and the solutions of mathematical are compared to experimental results. The grid size of 0.005 m is chosen for the current investigation since it requires less processing time due to a lesser number of elements.

Table 2
Mesh sensitivity analysis

Scenario	Grid size(m)	Grid per wave length	Total element in model	Transmission coefficient Ct
1	0.004	325	89756	0.61
2	0.005	260	71980	0.61
3	0.006	216	59455	0.70
4	0.007	185	52890	0.78
5	0.008	162	48434	0.81

4. Comparison of CFD Result and Experiments

Table 3 presents a statistical analysis of the output obtained from the CFD (Fluent solver) in comparison to experimental results. The Root Mean Square Error (RMSE) is utilized as a comparative metric. Equation contains the RMSE formula 8, Table 3 shows the statistical data obtained at different wave heights (0.10 m and 0.12 m) and submerge depths (0, 4, 7, 9, and 15 m). According to the statistical data, CFD outputs differed less from experimental results. Figure 11. Demonstrated the regression coefficient for observed and predicted data with regression approaches 88 %.

$$RMSE = \sqrt{\frac{1}{N}\sum_{i=1}^{N}(HNumerical - HExperimental)^2} \quad (9)$$

Table 3
Root Means Square Error (RMSE) of Fluent and Experiments

Parameters	Wave high	Submerged depth	Transmission wave (m)		RMSE
			CFD	Exp	
Wave characteristics	0.1 m	0	0.04	0.044	0.004
		4	0.036	0.041	0.005
		7	0.031	0.037	0.006
		9	0.026	0.030	0.004
		15	0.018	0.018	0.000
	0.12 m	0	0.048	0.045	0.003
		4	0.04	0.04	0.000
		7	0.036	0.039	0.003
		9	0.031	0.037	0.006
		15	0.021	0.019	0.003

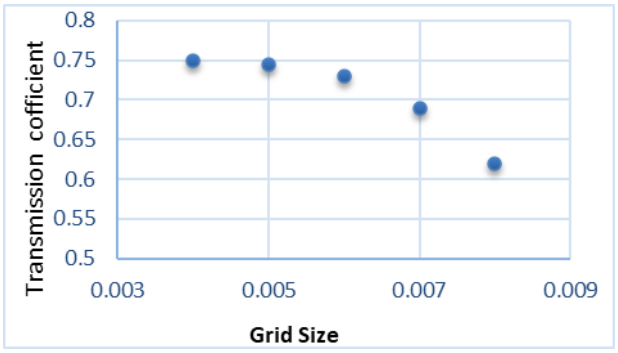

Fig. 10. Transmission coefficient variation for different grid sizes

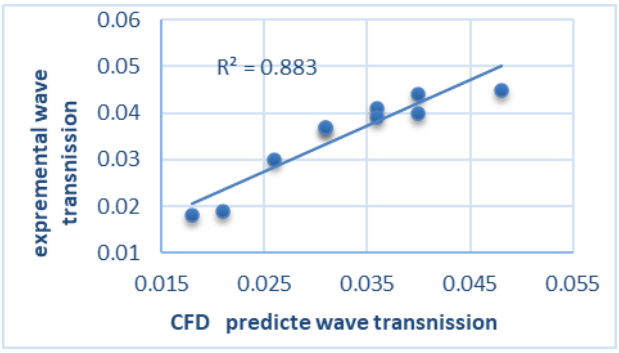

Fig. 11. Regression for observed and predicted data

5. Free Surface Profile (CFD and Experimental)

One of the real considerations for adopting the mathematical model is to verify the accuracy of the results drawn from this model by comparing it with the laboratory results. The attached figures (12, 13) show the compatibility of the experimental results and the mathematical model, by tracking the free flow surface for different models. We note from these previous figures a very large convergence between the mathematical model and the laboratory model.
Figure 14 shows the generation of waves in the CFD model at time 0 second to 8 second for different breakwater type. Figure 15 and 16 represent the turbulence intensity for different breakwater model, steps slope model makes the highest turbulence and dissipations more energy caused by eddy forms.

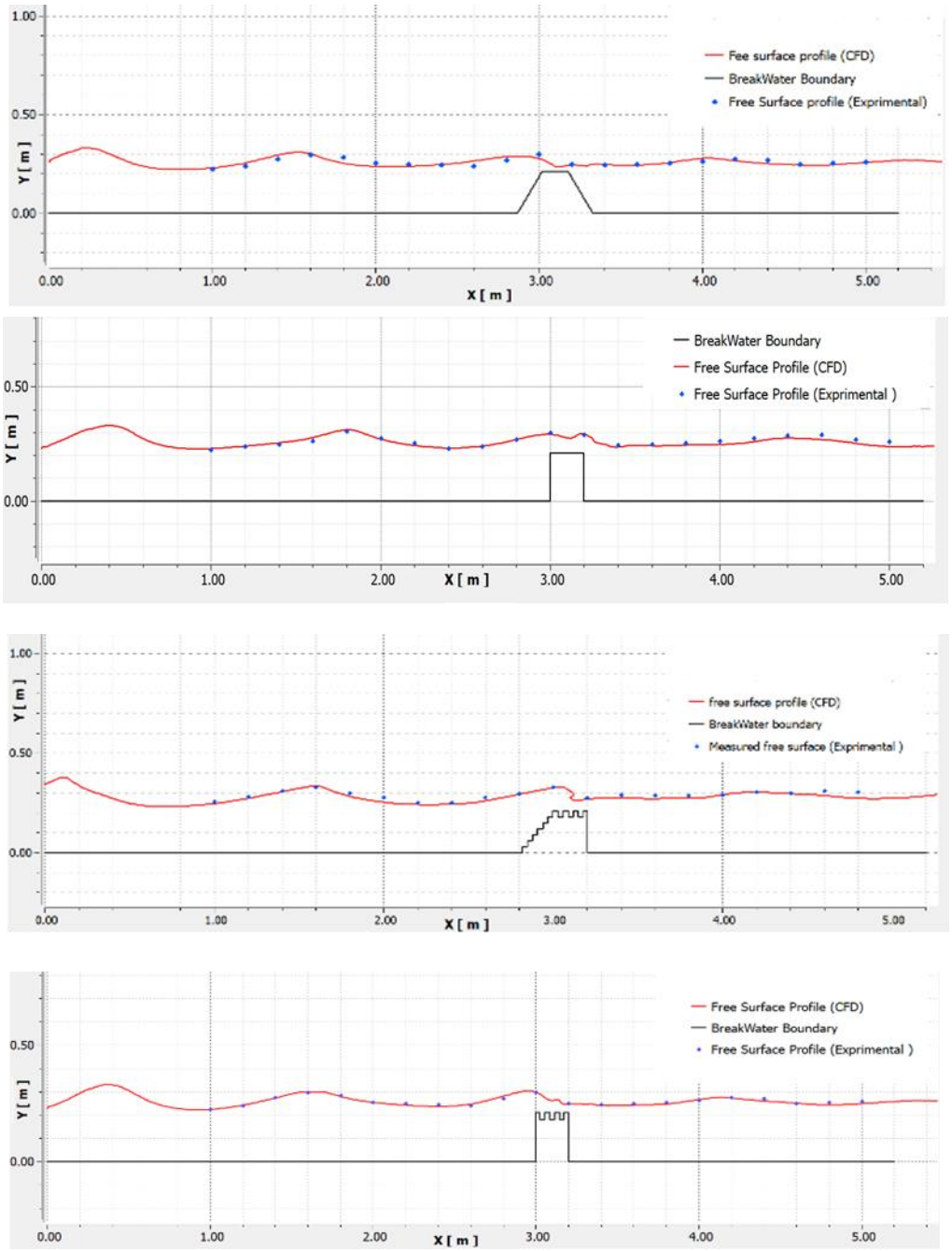

Fig. 12. Free surface profile for experimental and CFD results for different breakwater model

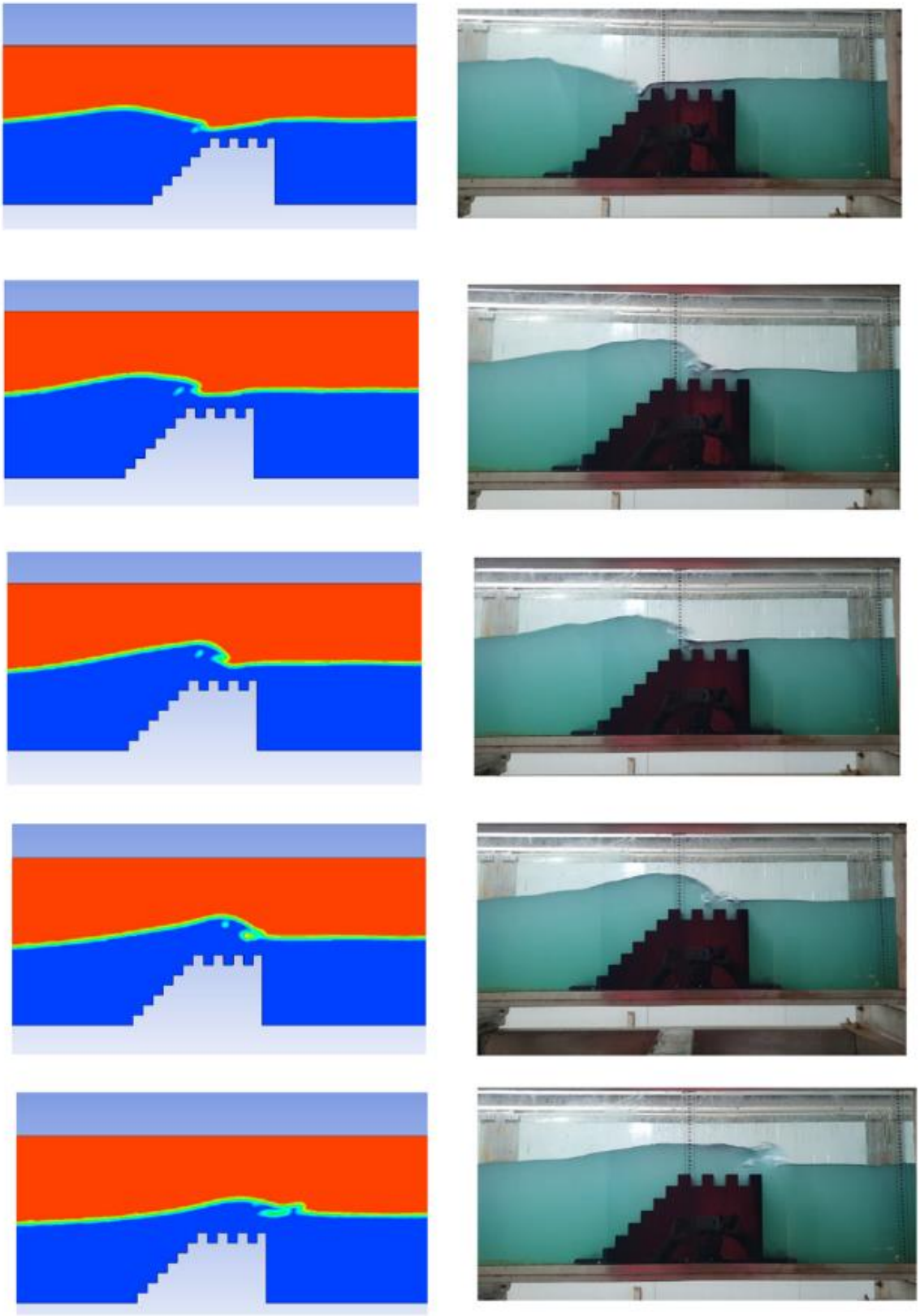

Fig. 13. Compassion for experimental and CFD model to represent the compatibility of result for flow time from 8.1 second to 8.5 second

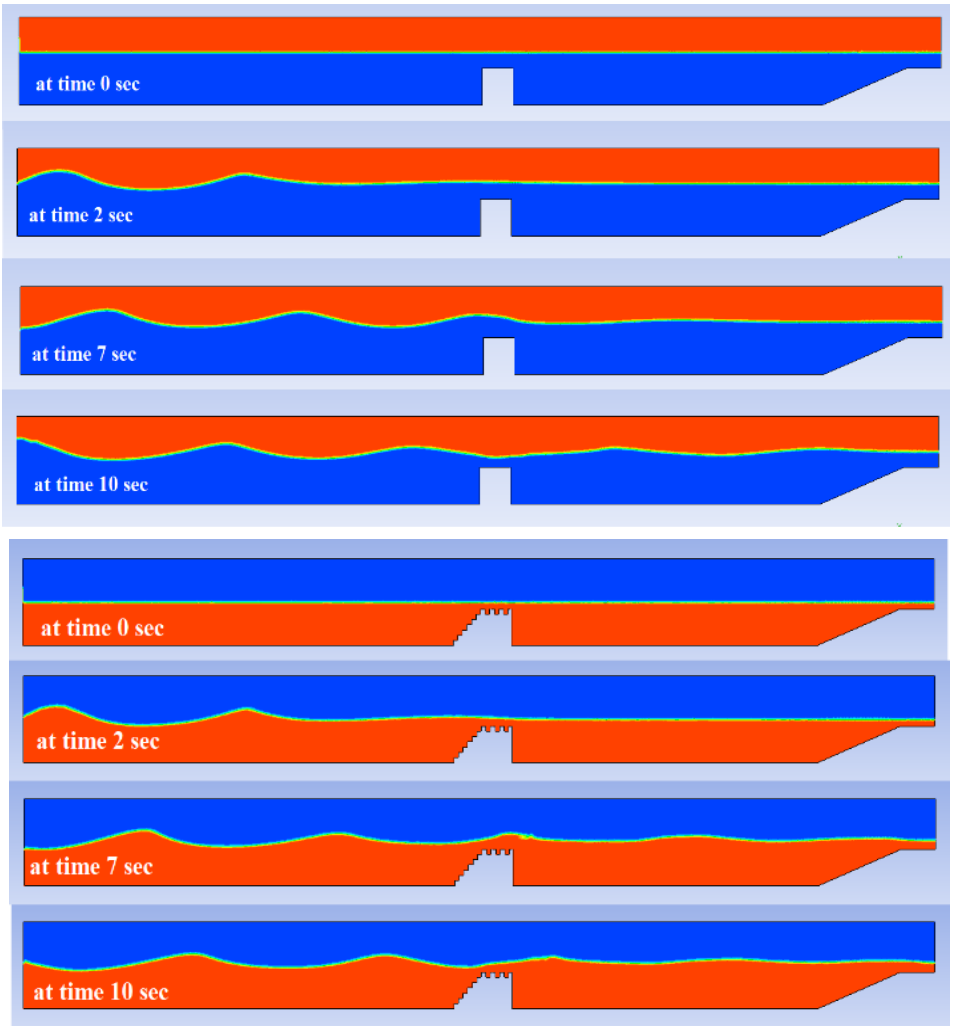

Fig. 14. Stages of wave generation for time series (time 0 sec to 10 sec)

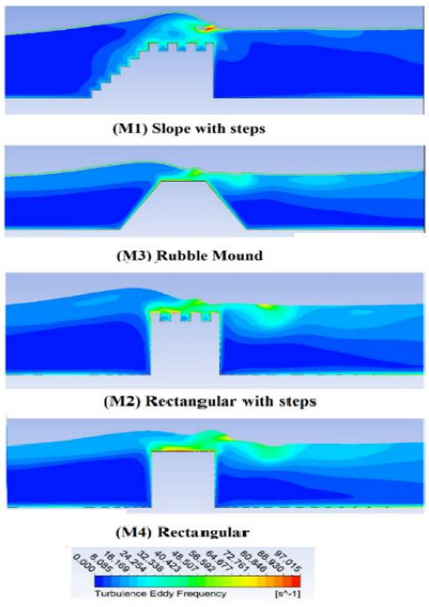

Fig. 15. Eddy turbulence frequency for different breakwater

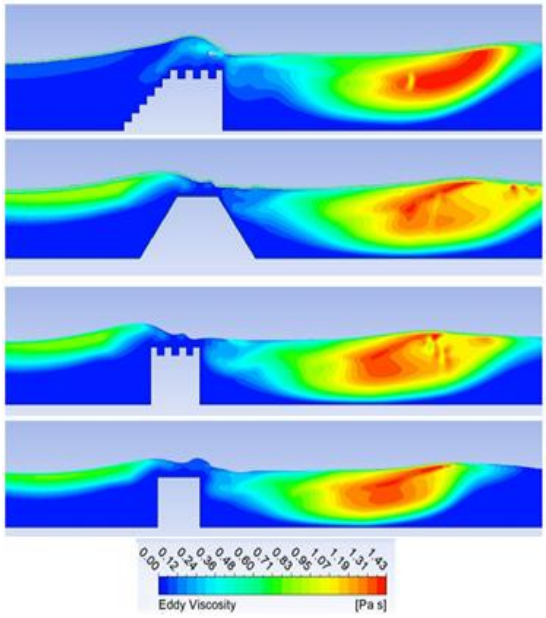

Fig. 16 eddy viscosity different breakwater pa.s

6. Different Hydraulic Waves Behaviour

One of the powerful features of CFD modelling is the graphical output of numerical variables, a small part of which represented in the following Figure 17. This figure represents different output of model M2 for different wave behaviour, velocity, eddy viscosity, turbulence frequency, pressure, and stream flow victor colour by celerity of wave.

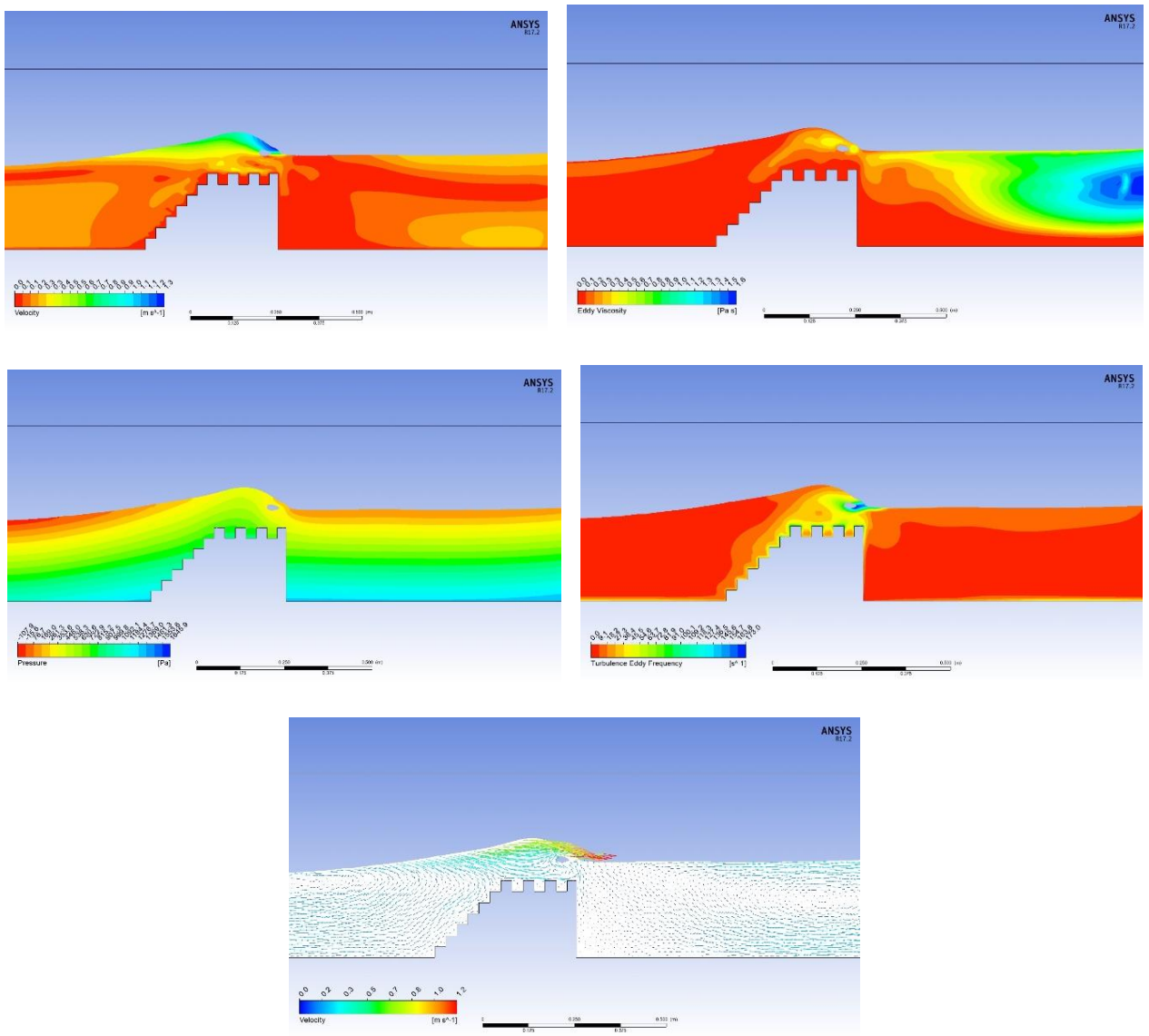

Fig. 17. Some off output results of CFD for model M2 (velocity, eddy viscosity, turbulence frequency, pressure, and stream flow victor colour by celerity of wave

7. Convergence of Solution and Stability

One of the most important criteria for accepting a numerical solution by CFD modelling is the arrival of the solution to the state of stability and convergence, which indicates that any addition or more time steps has very little or no effect on final results. Figure 18. Demonstrated the solution reach the limit of stability after 7000 iteration with time steps 0.01 sec.

Figure 19. Represent stages of free surface variations with wave period T is 1 sec and reach the stability after 7000 iteration with time steps 0.01 sec that reach 8.2 sec flow duration that make the wave characteristic identical.

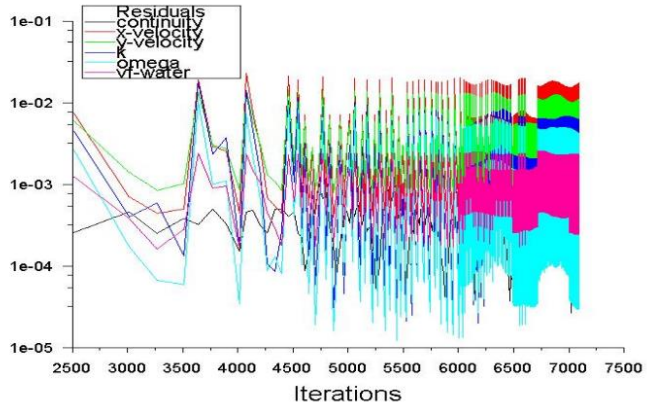

Fig. 18. Residuals verse iterations for solution converge

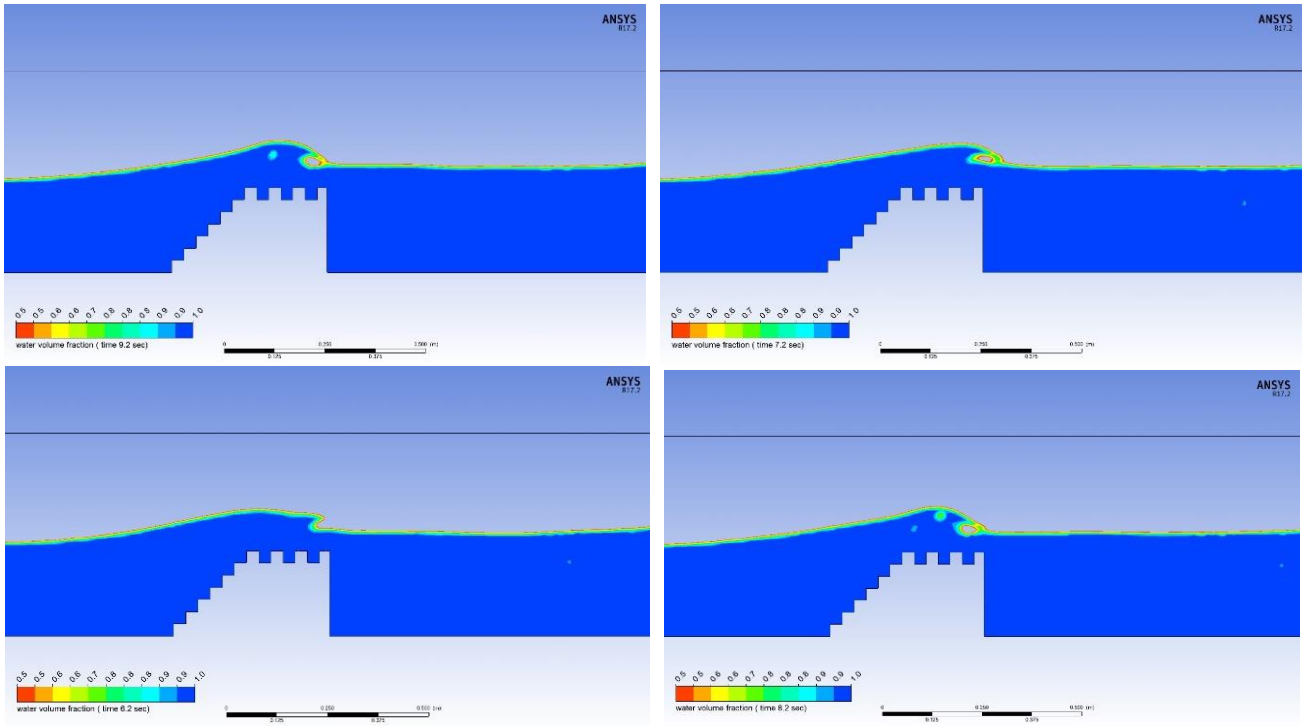

Fig. 19. demonstrated the variation in free surface during the time steps interval (reach the stability after 7000 iteration (8.2 sec)

8. Transmission Coefficient (Ct)

In this part of the research, Figures 20, 21, 22, 23 and 24, and Tables (4, 5, 6, 7, and 8) explain the variation in the value of the energy dissipation coefficient with respect the shapes of the breakwaters, as well as some variables related to the wave's characteristics are changed such as wave length and steepness.

It can be seen from these figures and tables, the maximum energy dissipation (1- Ct) (minimum transmission coefficient is received for sloped steps model M2, Figure 15 it is clear that the eddy turbulence frequency for M2 model are showed the more energy are disported at steps. The

minimum energy dissipation (1-Ct) (maximum transmission coefficient is received for narrow rectangular model M5.

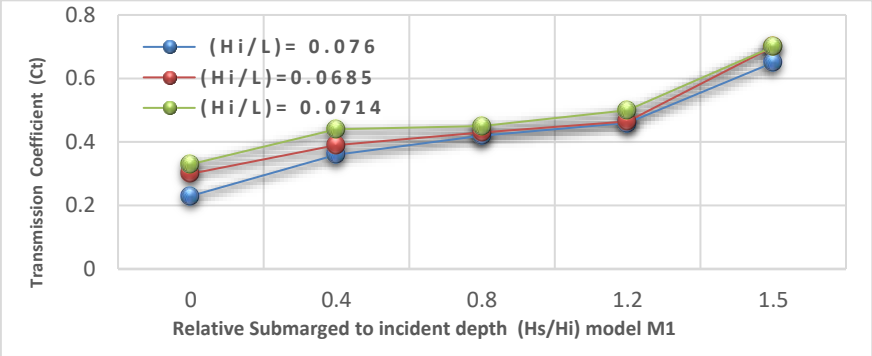

Fig. 20. variation of Ct according to wave steppes and relative submerged depth and Hi

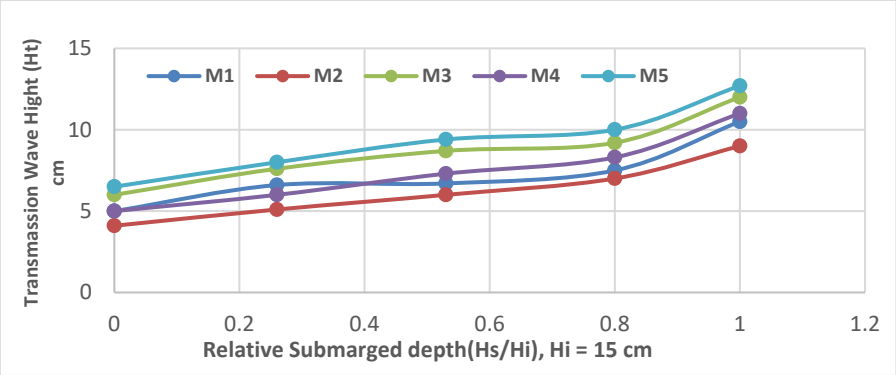

Fig. 21. variation of Ct according to wave steppes and relative submerged depth and Hi

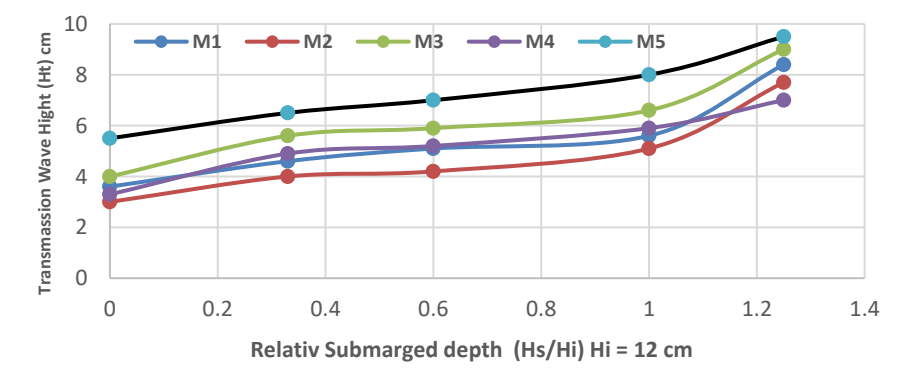

Fig. 22. variation of Ct according to wave steppes and relative submerged depth and Hi

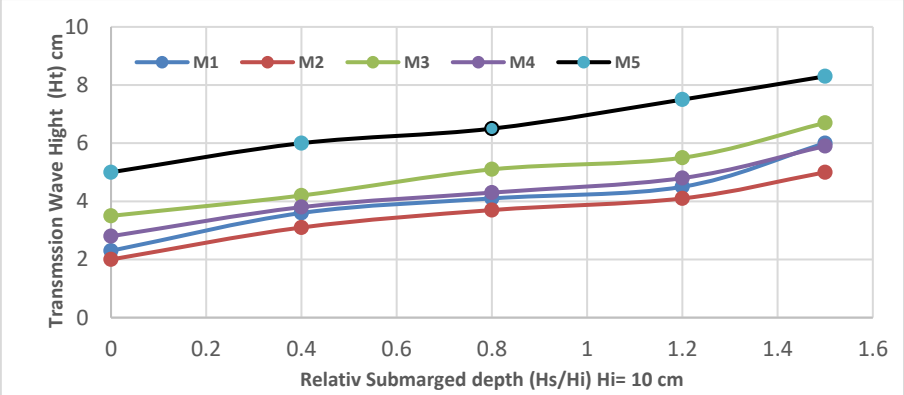

Fig. 23. variation of Ct according to wave steppes and relative submerged depth and Hi

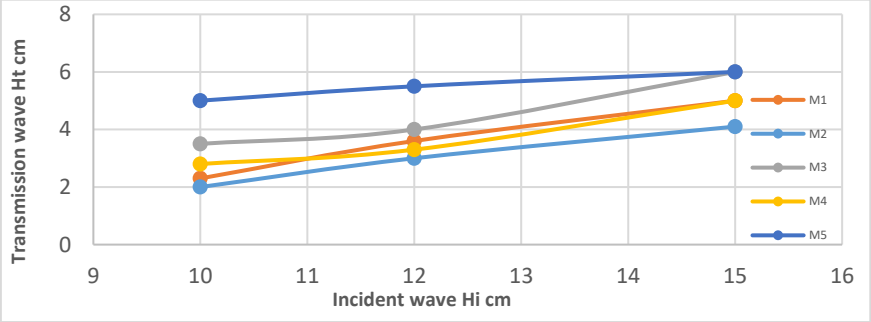

Fig. 24. Variation of Ht according to wave incident depth Hi

Table 4
Result of transmission coefficient (Ct) for different breakwater model (M1)

Model	RPM	Length of wave	Period T see	Experimental measurement					Transmission coefficient (Ct) =(Ht/Hi)	
				Wave steepness (Hi/L)	Hs	Hi	Hs/Hi	Ht	Experimental	CFD
M1 Rubble mound	30	1.3 m	0.75	0.0769	0	10	0	2.3	0.23	0.23
					4		0.4	3.6	0.36	0.33
					8		0.8	4.1	0.41	0.37
					12		1.2	4.5	0.45	0.41
					15		1.5	6	0.6	0.66
	35	1.75m	1	0.0685	0	12	0	3.6	0.3	0.26
					4		0.33	4.6	0.39	0.37
					8		0.6	5.1	0.43	0.39
					12		1	5.6	0.465	0.41
					15		1.25	8.4	0.7	0.66
	47	2.1 m	1.15	0.0714	0	15	0	5	0.33	0.39
					4		0.26	6.6	0.44	0.4
					8		0.53	6.7	0.45	0.39
					12		0.8	7.5	0.5	0.5
					15		1	10.5	0.7	0.73

Table 5
Result of transmission coefficient (Ct) for different breakwater model (M2)

Model	RPM	Length 0f wave	Period T see	Experimental measurement					Transmission coefficient (Ct) =(Ht/Hi)	
				Wave steepness (Hi/L)	Hs	Hi	Hs/Hi	Ht	Experimental	CFD
M2 Step sloped	30	1.3 m	0.75	0.0769	0	10	0	2.0	0.2	0.23
					4		0.4	3.1	0.31	0.33
					8		0.8	3.7	0.37	0.35
					12		1.2	4.1	0.41	0.39
					15		1.5	5	0.5	0.47
	35	1.75m	1	0.0685	0	12	0	3.0	0.25	0.26
					4		0.33	4.0	0.33	0.36
					8		0.6	4.2	0.35	0.32
					12		1	5.1	0.425	0.40
					15		1.25	7.7	0.64	0.61
	47	2.1 m	1.15	0.0714	0	15	0	4.1	0.27	0.25
					4		0.26	5.1	0.34	0.32
					8		0.53	6.0	0.4	0.36
					12		0.8	7.0	0.46	0.411
					15		1	9	0.6	0.56

Table 6
Result of transmission coefficient (Ct) for different breakwater model (M3)

Model	RPM	Length of wave	Period T see	Experimental measurement					Transmission coefficient (Ct) =(Ht/Hi)	
				Wave steepness (Hi/L)	Hs	Hi	Hs/Hi	Ht	Experimental	CFD
M3 Rectangular	30	1.3 m	0.75	0.0769	0	10	0	3.5	0.35	0.33
					4		0.4	4.2	0.42	0.39
					8		0.8	5.1	0.51	0.47
					12		1.2	5.5	0.55	0.52
					15		1.5	6.7	0.67	0.65
	35	1.75m	1	0.0685	0	12	0	4	0.33	0.29
					4		0.33	5.6	0.46	0.41
					8		0.6	5.9	0.49	0.45
					12		1	6.6	0.55	0.51
					15		1.25	9.0	0.75	0.69
	47	2.1 m	1.15	0.0714	0	15	0	6	0.4	0.4
					4		0.26	7.6	0.50	0.46
					8		0.53	8.7	0.58	0.53
					12		0.8	9.2	0.61	0.58
					15		1	12	0.8	0.72

Table 7
Result of transmission coefficient (Ct) for different breakwater model (M4)

Model	RPM	Length of wave	Period T see	Experimental measurement					Transmission coefficient (Ct) =(Ht/Hi)	
				Wave steepness (Hi/L)	Hs	Hi	Hs/Hi	Ht	Experimental	CFD
M4 Rectangle step	30	1.3 m	0.75	0.0769	0	10	0	2.8	0.28	0.24
					4		0.4	3.8	0.38	0.39
					8		0.8	4.3	0.43	0.43
					12		1.2	4.8	0.48	0.45
					15		1.5	5.9	0.59	0.53
	35	1.75m	1	0.0685	0	12	0	3.3	0.275	0.29
					4		0.33	4.9	0.41	0.45
					8		0.6	5.2	0.433	0.48
					12		1	5.9	0.5	0.51
					15		1.25	7	0.59	0.54
	47	2.1 m	1.15	0.0714	0	15	0	5	0.33	0.34
					4		0.26	6	0.4	0.44
					8		0.53	7.3	0.486	0.5
					12		0.8	8.3	0.55	0.56
					15		1	11	0.733	0.7

Table 8
Result of transmission coefficient (Ct) for different breakwater model (M5)

Model	RPM	Length of wave	Period T see	Experimental measurement					Transmission coefficient (C_t) =(Ht/Hi)	
				Wave steepness (Hi/L)	Hs	Hi	(Hs/Hi)	H_t	Experimental	CFD
M5 narrow Rectangular	30	1.3 m	0.75	0.0769	0	10	0	5	0.35	0.33
					4		0.4	6	0.42	0.39
					8		0.8	6.5	0.51	0.47
					12		1.2	7.5	0.55	0.52
					15		1.5	8.3	0.67	0.65
	35	1.75m	1	0.0685	0	12	0	5.5	0.33	0.29
					4		0.33	6.5	0.46	0.41
					8		0.6	7	0.49	0.45
					12		1	8	0.55	0.51
					15		1.25	9.5	0.75	0.69
	47	2.1 m	1.15	0.0714	0	15	0	6.5	0.4	0.4
					4		0.26	8	0.50	0.46
					8		0.53	9.4	0.58	0.53
					12		0.8	10	0.61	0.58
					15		1	12.7	0.8	0.72

9. Result and Discussion

The experimental results, in comparison with the numerical results, showed that the flume dimension (15*0.45*0.3) m used can be relied upon to represent the different breakwater models, in addition it is possible to avoid reflection of wave from faraway boundary through the use of a wave

absorber at the downstream side. It is essential to use UDF to describe the regular physical behaviour of the wave before reaching the breaker to ensure that no energy is lost from the wave before reaching breaker zone. Mesh independent solution is reached with a minimum of 240 grids per wave-length with a grid size 0.005 m and aspect ratio 1.
The increase in the surface area of the breakwater (steps breakwater) leads to an increase in the dissipations of the incident wave energy through the generation of turbulence and vortices at the front of the breaker. As a result, and Briefly:

i. Transmission coefficient are increased with increased of incident wave high for all type of breakwater model.
ii. The highest value for energy dissipations (1 - Ct) % are received for zero submerged depth in model of sloped steps model (M2) is 80 %.
iii. The minimum energy dissipation (1-Ct) % (maximum transmission coefficient is received for narrow rectangular model M5 is
iv. For all models of breakwater, transmission wave height (Ht) are increased with increased relative submerged depth (Hs/Hi).
v. The non-uniformity of the steps located in front of the breakwater structure effectively contributes to the dissipation of incident wave energy, resulting in a notable reduction in transmitted wave height at the coastal area.

Acknowledgement
This research was not funded by any grant.

References:

[1] Bilici, Çağdaş. "A Model study on wave transmission through pile breakwaters." Master's thesis, Middle East Technical University, 2014. https://doi.org/10.9753/icce.v34.posters.18
[2] Harris, Lucy. "MPM study of water wave interaction with porous seawalls." PhD diss., University of Cambridge, 2020.
[3] Takahashi, Shigeo. Design of vertical breakwaters. PARI (Port and Airport Research Institute, 2002.
[4] Dean, Robert G., and Robert A. Dalrymple. Water wave mechanics for engineers and scientists. Vol. 2. world scientific publishing company, 1991. https://doi.org/10.1142/1232
[5] Abdul Khader, M. Ii, and S. P. Rai. "A study of submerged breakwaters." *Journal of Hydraulic Research* 18, no. 2 (1980): 113-121. https://doi.org/10.1080/00221688009499555
[6] Douglass, Scott L., and Joe Krolak. *Highways in the coastal environment: Hydraulic engineering circular 25*. No. FHWA-NHI-07-096. United States. Federal Highway Administration. Office of Bridge Technology, 2008.
[7] Dick, T. Milne, and A. Brebner. "Solid and permeable submerged breakwaters." In *Coastal Engineering 1968*, pp. 1141-1158. 1968. https://doi.org/10.1061/9780872620131.072
[8] Seabrook S. R. and Hall K. R., "Wave Transmission at Submerged Rubble Mound Breakwaters", COASTAL ENGINEERING, CHAPTER, (1998).
[9] Calabrese, M., Diego Vicinanza, and M. Buccino. "Low-crested and submerged breakwaters in presence of broken waves." In *Proceedings of HYDRALAB-II, Budapest, Hungary*. 2003. https://doi.org/10.1142/9789812791306_0160
[10] Tajziehchi, Mojtaba. "Experimental and numerical modelling of wave-induced current and wave transformation in presence of submerged breakwaters." PhD diss., UNSW Sydney, 2006.
[11] Liao, Yi-Chun, Jyun-Han Jiang, Yi-Ping Wu, and Chung-Pan Lee. "Experimental study of wave breaking criteria and energy loss caused by a submerged porous breakwater on horizontal bottom." *Journal of Marine Science and Technology* 21, no. 1 (2013): 5.
[12] Replumaz, Alexis, Yann Julien, and Damien Bellengier. "Concrete Breakwater for the Greater Tortue Ahmeyim Project for BP in Mauritania and Senegal." In *Offshore Technology Conference*, p. D032S085R013. OTC, 2021. https://doi.org/10.4043/30534-MS
[13] Al Shaikhli, Hasan Ibrahim, and Saleh Issa Khassaf. "Stepped Mound Breakwater Simulation by Using Flow 3D." *Eurasian Journal of Engineering and Technology* 6 (2022): 60-68.

[14] Hsu, Tai-Wen, Chih-Min Hsieh, and Robert R. Hwang. "Using RANS to simulate vortex generation and dissipation around impermeable submerged double breakwaters." *Coastal Engineering* 51, no. 7 (2004): 557-579. https://doi.org/10.1016/j.coastaleng.2004.06.003
[15] Zhang, J-S., D-S. Jeng, PL-F. Liu, C. Zhang, and Y. Zhang. "Response of a porous seabed to water waves over permeable submerged breakwaters with Bragg reflection." *Ocean Engineering* 43 (2012): 1-12. https://doi.org/10.1016/j.oceaneng.2012.01.024
[16] Young, D. Morgan, and Firat Y. Testik. "Wave reflection by submerged vertical and semi-circular breakwaters." *Ocean Engineering* 38, no. 10 (2011): 1269-1276. https://doi.org/10.1016/j.oceaneng.2011.05.003
[17] Liao, Yi-Chun, Jyun-Han Jiang, Yi-Ping Wu, and Chung-Pan Lee. "Experimental study of wave breaking criteria and energy loss caused by a submerged porous breakwater on horizontal bottom." *Journal of Marine Science and Technology* 21, no. 1 (2013): 5.
[18] Hajivalie, Fatemeh, and Seyed Masoud Mahmoudof. "Experimental Study of Energy Dissipation at Rectangular Submerged Breakwater." Proc. of ICFM8. Sendai, Japan (2018).
[19] Ringe, Shivansh. "Designing of One Directional Wave Tank." (2020).
[20] Abobaker, M., Addeep, S., Afolabi, L. O., & Elfaghi, A. M. "Effect of Mesh Type on Numerical Computation of Aerodynamic Coefficients of NACA 0012 Airfoil. " *Journal of Advanced Research in Fluid Mechanics and Thermal Sciences* 87, no. 3 (2021): 31-39. https://doi.org/10.37934/arfmts.87.3.3139
[21] Poguluri, Sunny Kumar, and I. H. Cho. "Wave dissipation over a horizontal slotted plate with a leeside vertical seawall: analytical and numerical approaches." *Coastal Engineering Journal* 63, no. 1 (2021): 52-67. https://doi.org/10.1080/21664250.2020.1850396
[22] ANSYS, Inc. ANSYS FLUENT User's Guide, Southpointe 277 Technology Drive Canonsburge PA 15317; USA, 2010.
[23] Osman, M. S., J. A. T. Machado, and Dumitru Baleanu. "On nonautonomous complex wave solutions described by the coupled Schrödinger–Boussinesq equation with variable-coefficients." *Optical and Quantum Electronics* 50 (2018): 1-11. https://doi.org/10.1007/s11082-018-1346-y
[24] Novak, Pavel, Vincent Guinot, Alan Jeffrey, and Dominic E. Reeve. *Hydraulic modelling: An introduction: Principles, methods and applications*. CRC Press, 2018.
[25] Sharifahmadian, Amir. *Numerical models for submerged breakwaters: coastal hydrodynamics and morphodynamics*. Butterworth-Heinemann, 2015.